

Systematic long-term comparison of spectral UV measurements and UVSPEC modeling results

B. Mayer and G. Seckmeyer

Fraunhofer Institute for Atmospheric Environmental Research, Garmisch-Partenkirchen, Germany

A. Kylling

NORUT Information Technology, Tromsø, Norway

Abstract. For the evaluation of radiative transfer models and for investigations on the influence of parameters like aerosols or clouds on ground level UV irradiance, a combination of spectral measurements and model calculations is required. We show an efficient method for such a combination and present a systematic comparison of the freely available UVSPEC radiative transfer model package with two years of spectrally resolved measurements made at Garmisch-Partenkirchen, Germany (47.48°N, 11.07°E, 730 m above sea level) for cloudless sky and low albedo. More than 1200 spectra have been used for the comparison, covering a wide range of ozone and aerosol conditions. Applying the PSEUDO-SPHERICAL model type, a discrete ordinate model with correction for the sphericity of the Earth, the systematic differences between measurement and model were found to range between -11 and +2% for wavelengths between 295 and 400 nm and solar zenith angles up to 80°. The small observed statistical differences of 2-3% can mostly be explained by the random error of the measurement system. Only two input parameters, total ozone column and aerosol optical depth, the latter parameterized by the Ångström formula, are required to reach this level of agreement. It was further found that knowledge of the aerosol optical depth is essential for obtaining such a good agreement. The evaluated UVSPEC model package, together with the presented interface SDMODEL, provides an efficient tool for the investigation of the processes that control surface UV irradiance.

1. Introduction

Changes in the ozone column are known to result in changes in the UVB irradiance reaching the Earth's surface. The observed decrease of stratospheric ozone concentrations [Harris *et al.*, 1995] should therefore be connected with an increase of harmful UV irradiance. While the relationship between total ozone column and UV is well established [McKenzie *et al.*, 1995], the influence of other parameters like aerosols and clouds is in the focus of current research. For the prediction of future UV changes all these parameters have to be considered rather than total ozone column alone. Increases in (man-made) aerosols or cloudiness may for example counteract ozone-related trends. In order to predict future developments of UV surface irradiance, radiative transfer models are needed which consider all these parameters.

The main fields of application for radiative transfer models are (1) to calculate past and future UV levels for risk assessments on the basis of estimated trends of ozone, aerosol distribution and cloud cover; (2) to perform process studies, that is, to investigate the influence of atmospheric parameters on surface irradiance (e.g., the study of attenuation by aerosols comparing measured and modeled aerosol-free spectra); and (3) to model the radiation at places, times and situations where measurements are not possible or not available (models could in this context be used as an interpolation between a very sparse network of measurement sites). For all these applications it would be desirable to achieve the most accurate results with the smallest possible set of input parameters. The latter should be easily available like, e.g., the total ozone column and atmospheric visibility. One of the aims of comparisons between experimental and model data is to find out an optimum set of input parameters.

Various models are available to date, a rather large fraction of which are based on the one-dimensional radiative transfer solver by Stamnes *et al.* [1988]. One of these is the freely available UVSPEC model package. Similar to measurements, models are subject to

several uncertainties. These may be divided into two classes: numerical errors and uncertainties in the input data. While numerical errors are avoidable by thorough programming and testing, the latter can only be investigated by sensitivity studies and by comparing model results with measured data. This second type comprises uncertainties in the input data (e.g., the extraterrestrial irradiance or the absorption cross section of ozone) and imperfections in the parameterization of the atmosphere. A full description of the atmosphere by means of a phase function specified at any given location is neither possible nor practical. Rather, a parameterization using only a few parameters is necessary. Furthermore, simplifying assumptions are made in order to obtain a tractable solution of the radiative transfer equation, e.g., one-dimensional model atmosphere geometry. The arising uncertainties can only partly be investigated by sensitivity studies with models alone [Ruggaber *et al.*, 1994]. Comparison with experimental data is necessary to quantify the actual size of the uncertainties. It should be noted that these studies require sufficient data for the description of the atmosphere in addition to the spectral measurements.

Although comparisons with experimental data are necessary to estimate the accuracy and applicability of a model, only a few such studies have been carried out up to now and these are mostly restricted to the description of single spectra or diurnal variations. Forster *et al.* [1995] compared measurements with calculations from their own radiative transfer model. In the UVB, the measured data were found to be higher than the model values. Generally, such an observation may be explained by a stray light problem of the monochromator. In a different case study, Wang and Lenoble [1994] describe a comparison between their radiative transfer model and data of two instrument intercomparisons [Gardiner *et al.*, 1993; Gardiner and Kirsch, 1993]. While the variation of the ratio between measurement and model exceeds $\pm 20\%$, the agreement is better than $\pm 6\%$ when the ratio is averaged over intervals of 10 nm. Koskela and Taalas [1993] used a modified earlier version of UVSPEC in comparison with measurements from a spectroradiometer of the single Brewer type. The systematic deviation exceeded 40% between 300 and 325 nm, while the agreement with data from the National Science Foundations network at Palmer Station (Antarctica) was quite good. Finally, Zeng *et al.* [1994] used the ratio between direct and diffuse irradiance for their comparison. This parameter is not subject to the uncertainties of the extraterrestrial irradiance and the absolute calibration of the spectroradiometer, but is very sensitive to aerosol optical depth and surface albedo. Therefore, this ratio is a very useful parameter to study the influence of aerosol optical depth and the profiles of aerosol extinction and ozone. It is interesting to note that all the models used in these studies are based on the radiative transfer equation solver of Stamnes *et al.* [1988].

An evaluation of a model requires a wide variety of atmospheric conditions and should contain at least 1 year of measurements to cover all typical situations.

To our knowledge, the present study is the first complete evaluation of a model at a particular site comprising 1200 cloudless sky spectra sampled over two years (April 1994 to March 1996). The cloudless sky is a very important case for two reasons: (1) cloudless sky is connected with comparatively high irradiance levels; and 2) many applications require modeled cloudless sky irradiance. The most important input parameters during cloudless skies and snow-free ground, total ozone column and spectral aerosol optical depth, are available at our site from measurements of direct spectral irradiance. An appropriate interface between measurement and model has been developed in order to enable the extensive comparison for several model types. The scope of the present investigation is not only to show the results of this comparison, but also to introduce the methods that can be used to perform such a comparison.

2. Materials and Methods

2.1. Measurement System

The spectroradiometric system used for the investigation is situated on the roof platform of the Fraunhofer Institute for Atmospheric Environmental Research (IFU) in Garmisch-Partenkirchen (47.48°N , 11.07°E , 730 m above sea level). It serves as a stationary weatherproof reference instrument and comprises a Bentham double monochromator DTM 300 with a photomultiplier as detector. Spectra of global irradiance are taken with a quartz cosine diffuser, and direct spectral irradiance is measured with a narrow field-of-view entrance optics, which is automatically aligned to the Sun. Both optics are coupled to the entrance slit of the monochromator with quartz fiber bundles. The angular response of the quartz diffuser is well known from laboratory studies; the deviation from the ideal cosine response is corrected using an algorithm described by Seckmeyer and Bernhard [1993] (the correction factors range between 1.05 for high Sun and 1.1 for low Sun). To avoid errors arising from changes in the photomultiplier dark current, we use an optical chopper in conjunction with a lock-in technique. The whole system is maintained at $(20 \pm 0.5)^{\circ}\text{C}$ and has an independent power supply. Calibrations are carried out in situ at least once a week using 100 W tungsten-halogen standard lamps. With a spectral resolution of 0.6 nm and a step width of 0.25 nm between 285 and 410 nm, approximately 100 spectra are taken every day with a typical scan duration of 10 min for this wavelength range. If the Sun is visible, spectra of direct and global irradiance are sampled alternatingly; otherwise, only global spectra are measured. Data are stored in so-called solar databases which hold not only the wavelength and the spectral irradiance, but also the time of the measurement, the raw data, and the statistical error for every single data point. The instrument has performed well in several intercomparisons of spectroradiometers [Seckmeyer *et al.*, 1994; Gardiner and Kirsch, 1995; Seckmeyer *et al.*, 1995]. Further instrumental details are given by Seck-

meyer et al. [1996]. The spectral measurements are supplemented with several ancillary sensors for quality control purposes, and to provide complementary information. They comprise, among others, a global irradiance pyranometer, a direct Sun pyranometer mounted on a Sun-tracking system, and two Robertson-Berger type meters [*Mayer and Seckmeyer, 1996*].

For the comparison of measured and modeled data, site information is essential. The IFU is located in a valley at the northern boundary of the Bavarian Alps. The horizon is formed by the surrounding mountains which do not exceed 20° measured from the horizontal direction. The highest elevations are to the south and north; the east and west are nearly free. In order to consider the decrease in irradiance due to shading by mountains, the line of the horizon was measured. The fraction of cosine-weighted area of the sky which is covered by mountains is 3.8%. To correct for this effect, the diffuse model irradiance was reduced by 3.8%, assuming that the sky radiance can be considered isotropic in the UV range, as a first approximation. This assumption is not completely justified in the UVA [*Blumthaler et al., 1996*], but with respect to the small absolute value of the correction (between 1.9 and 3.8%, depending on the ratio of diffuse to global irradiance) the introduced uncertainty is quite small.

Comparisons between modeled and measured data require an adequate description of the atmosphere. The most important parameters for modeling cloudless sky irradiance are ozone column, spectral aerosol optical depth, surface pressure and albedo. The first two parameters can be derived from measurements of the spectral direct irradiance, while the experimental determination of the surface albedo is very complicated in an area as inhomogeneous as the surroundings of the IFU site. For the present study, however, periods with snow-covered surface have been excluded from the analysis. The albedo was chosen to be 0.02, following measurements of *Blumthaler and Ambach [1988]* for various surfaces. Total ozone column and spectral aerosol optical depth have been calculated with the DSI (direct spectra interpretation) algorithm which is described in the appendix. While DSI provides UV aerosol optical depth using the Ångström parameterization, the original UVSPEC distribution requires the meteorological visibility R_m for the description of the aerosols. If not available at a site, visibility can be estimated from the Ångström parameters α and β using a formula by *Iqbal [1983]*:

$$\begin{aligned} \beta \cdot 0.55^{-\alpha} &= \left(\frac{3.912}{R_m[\text{km}]} - 0.01162 \right) \\ &\cdot [0.02472 \cdot (R_m[\text{km}] - 5) + 1.132] \end{aligned} \quad (1)$$

It should be noted, however, that the visibility may provide a good parameterization in the visible range, but has its limitations in the UV. In order to calculate aerosol optical depth in the UV range, an additional assumption about the wavelength dependence is

required for the necessary extrapolation from the visible (comparable to the Ångström parameter α). Visibility, however, is a useful model input parameter insofar as it is available at many sites. A better description in the UV range is provided by the Ångström parameters themselves, a fact which has been accounted for with a model change described below.

2.2. Selection of Cloudless Sky Situations

The cloudless sky spectra used for this investigation were selected according to the global and direct Sun pyranometers, the signals of which are sampled in 1-min intervals. These can be used to estimate whether the sky is free of clouds or not, even if no independent cloud observations are available. Fast variations of direct and global irradiance in time are always due to clouds or contrails. Therefore we chose only intervals where the fast variations of the direct and global irradiance on the 1-min scale were less than ±1% for a minimum time of 1 hour. The possibility still exists that some situations with little cloud cover are included in the analysis, which, in the worst case, might slightly enlarge the statistical uncertainty in the comparison of model and measurement. In the results section we show that this is not the case.

2.3. UVSPEC: The Model

UVSPEC is a freely available software package for calculation of diffuse and direct UV and visible irradiances and radiances at any altitude. The wavelength range from 176.0 nm to 850.0 nm is covered with a resolution of 1.0 nm. Optional cloud and aerosol models may be included.

The UVSPEC package comprises three different radiative transfer solvers: (1) the general purpose discrete ordinate algorithm DISORT for transfer calculations in vertically inhomogeneous, nonisothermal plane-parallel media [*Stamnes et al., 1988*], which can be used to calculate the irradiance, radiance, flux divergence, and mean intensity; (2) a SPHERICAL and a PSEUDO-SPHERICAL version of DISORT which introduce corrections for the sphericity of the Earth; they are implemented as described by *Dahlback and Stamnes [1991]* and may be used to calculate the irradiance, radiance, flux divergence, and mean intensity; and (3) the two-stream algorithm TWOSTREAM for radiative transfer in vertically inhomogeneous, plane-parallel or pseudo-spherical, layered media [*Kylling et al., 1995*], which may be used to calculate the irradiance, flux divergence, and mean intensity. Computing time and accuracy are quite different for these model types.

The calculation of the downward welling irradiance is normally split in two; the calculation of the direct irradiance and the calculation of the diffuse irradiance. The direct irradiance is calculated by the Bouguer-Lambert-Beer law. For the spherical radiative transfer solvers the optical path is calculated in spherical geometry. In order to calculate the diffuse irradiance, it is sufficient to solve the azimuthally averaged radiative transfer equation, e.g. [*Lenoble, 1993*]

$$\begin{aligned}
 -\mu \frac{dI(\tau, \mu)}{d\tau} = & -I(\tau, \mu) \\
 & + \frac{\omega(\tau)}{2} \int_{-1}^1 p(\tau, \mu, \mu') I(\tau, \mu') d\mu' \\
 & + \frac{\omega(\tau)}{4\pi} p(\tau, \mu, -\mu_0) E_0 e^{-\tau/\mu_0}. \quad (2)
 \end{aligned}$$

The first term on the right-hand side represents extinction, the second represents multiple scattering and the third represents the direct beam source. Here $I(\tau, \mu)$ is the radiance at optical depth τ in the direction μ , where $\mu = \cos \theta$, and θ is the polar angle. Furthermore, $p(\tau, \mu, \mu')$ is the phase function for scattering from direction μ' to μ , $\omega(\tau)$ the single-scattering albedo and E_0 the extraterrestrial solar flux incident at the solar zenith angle $\theta_0 = \cos^{-1} \mu_0$. Equation (2) describes the diffuse radiative transfer in a plane-parallel atmosphere. The plane-parallel approximation is valid for solar zenith angles smaller than about 70° . For larger solar zenith angles the curvature of the Earth's atmosphere must be considered. In the pseudo-spherical approximation this is done by making the substitution

$$e^{-\tau/\mu_0} \rightarrow e^{-ch(\tau, \mu_0)} \quad (3)$$

in the direct beam source term of equation (2). Here $ch(\tau, \mu_0)$ is the Chapman function calculated according to *Dahlback and Stamnes* [1991], who also discussed the accuracy of the pseudo-spherical approximation. The accuracy is sufficient for the solar zenith angles encountered in this study.

None of the radiative transfer solvers used here accounts for polarization. However, for the calculation of angularly integrated radiative quantities like the global irradiance, polarization effects are small and therefore negligible.

When numerically solving equation (2), a compromise between speed and accuracy has to be found. With the discrete ordinate method the number of streams used to approximate the integral in equation (2) largely controls the computing time [*Stamnes et al.*, 1988]

$$\int_{-1}^1 \rightarrow \sum_{\substack{i=-n \\ i \neq 0}}^n \text{ or } \sum_{\substack{i=1 \\ i \neq 0}}^1 \quad (4)$$

where the first summation is for the multistream case and the second for the two-stream case. Here $2n$ is the number of streams, where $n \geq 1$. The multistream algorithms include the two-stream approximation as a special case. However, specially designed two-stream algorithms are generally much faster than multistream algorithms run in the two-stream mode. The pseudo-spherical radiative transfer equation solver used extensively in this study was run with $n = 5$, i.e., in 10-stream mode.

The inputs to the radiative transfer solvers are the optical depths, single scattering albedos and phase functions of each atmospheric layer [*Stamnes*, 1986]. Additionally, the surface albedo and an extraterrestrial solar spectrum must be specified. The optical depth for ozone

was calculated using the temperature dependent ozone absorption cross section from *Daumont et al.* [1992] and the U.S. standard atmosphere [*Anderson et al.*, 1986]. The ozone profile was scaled to match the input parameter total ozone column. The Rayleigh scattering cross section was calculated with the formula given by [*Nicolet*, 1984] and the Rayleigh phase function was utilized. For the aerosols the appropriate spring/summer and fall/winter background aerosol models of *Shettle* [1989] were used, employing a Henyey-Greenstein phase function. In this parameterization, the aerosol optical depth at each layer is determined from the input parameter visibility.

The extraterrestrial irradiance used in this study was measured by the Solar Ultraviolet Spectral Irradiance Monitor (SUSIM) on board the Space Shuttle during the ATLAS 3 mission in November 1994 (M.E. Van-Hoosier, personal communication, 1996). The spectrum has been shifted to air wavelengths using a formula provided by *Teillet* [1990], because the wavelength calibration of our measurements also refers to air wavelengths (this shift is between 0.08 and 0.11 nm, depending on the wavelength).

2.4. Modification of the Original UVSPEC Version

Some modifications to the UVSPEC radiative transfer model described in the last section have been introduced. They resulted in a new model type, TWODIS, which combines the benefits of TWOSTREAM and PSEUDO-SPHERICAL and an enhanced model version which uses the Ångström parameterization of aerosol optical depth instead of the visibility.

2.4.1. TWODIS model. TWOSTREAM and PSEUDO-SPHERICAL both have advantages, the former in speed, the latter in accuracy. Our intention was to combine the positive features of both to create a fast and accurate model. In order to achieve this aim, we investigated their systematic differences as a function of solar zenith angle, ozone column and visibility. According to earlier investigations [*Kylling et al.*, 1995], the deviations between both model types are less than 10% for low albedo and solar zenith angles below 60° . Our new calculations showed that the difference mainly depends on solar zenith angle and only to a lower degree on ozone column and aerosol optical depth. The ratio of both model types therefore can be specified as a function of solar zenith angle and wavelength in good approximation. In order to correct the TWOSTREAM model we calculated the ratio between the model types in steps of 1 nm and 5° for an average ozone column of 320 Dobson Units (DU) and an aerosol-free atmosphere; the results were stored in a table. The mathematical formulation for the so defined model type TWODIS can be described as:

$$\begin{aligned}
 \text{TWODIS} := & \text{TWOSTREAM}(d, R_m, A, \theta, \lambda) \cdot \\
 & \left[\frac{\text{PSEUDO-SPHERICAL}(320 \text{ DU}, 200 \text{ km}, 0, \theta, \lambda)}{\text{TWOSTREAM}(320 \text{ DU}, 200 \text{ km}, 0, \theta, \lambda)} \right]
 \end{aligned} \quad (5)$$

where d is the total ozone column, R_m the meteorological visibility, A the ground albedo and θ the solar zenith angle. The tabulated values (expression in brackets in equation (5)) are interpolated to the given solar zenith angle and wavelength. Spectra calculated with TWODIS are comparable to PSEUDO-SPHERICAL with respect to accuracy and to TWOSTREAM with respect to the required processor time. TWODIS can be used whenever huge amounts of model calculations are required, e.g., to calculate model values for a month or even a year of measurements. For process studies, however, we prefer PSEUDO-SPHERICAL, which provides the physically more correct description.

2.4.2. Aerosol Parameterization Using Ångström Turbidity. In order to make the best use of the aerosol parameterization which is available at the IFU site, UVSPEC was modified to accept the Ångström parameters α and β directly instead of the visibility which previously had to be estimated using equation (1). This is achieved by initially calculating the aerosol optical depth profile according to Shettle [1989] from the estimated visibility (like in the original UVSPEC package) and re-scaling the first two kilometers of this profile afterwards, in order to get the specified Ångström optical depth in total. The scaling is done only for the first two kilometers, because most of the atmospheric aerosol is concentrated in this layer.

Thus a modified (++) version was created for each of the UVSPEC model types. The comparison with measurements in the results section clearly shows the advantage of this parameterization, especially when looking at the direct irradiance which is much more sensitive to variations in the aerosol optical depth than the global irradiance.

2.5. SDMODEL: The interface

In order to facilitate systematic comparisons for large amounts of data, SDMODEL (solar database modeling interface) has been developed as a general interface between modeled and experimental spectra. The technical environment for gathering experimental data is in general quite different from the ideal assumptions of models. Besides the simplified description of the atmosphere, these aspects of the technical environment include the bandwidth of the measurement system and the time interval necessary to gather a complete spectrum. Neglecting the difference in bandwidth leads to a large scatter in the ratio of measurement and model. Considering the different bandwidths of the measurement system and the model, the most convenient way is to convolute the model spectrum with the slit function of the monochromator. It has to be kept in mind that this may introduce errors if the bandwidth of the monochromator is too large. The required time to measure a spectrum leads to a difficulty in the comparison of data: While a measured spectrum is subject to changes of solar zenith angle and atmospheric conditions during the scan time, a model usually assumes these parameters to remain constant for a given spectrum (even if the calculation time may considerably exceed the mea-

surement time). In principle, there are two ways to overcome this problems: (1) adapt the measured data to the model; that entails interpolating spectra to specified times and deconvoluting the measured spectra using the slit function of the monochromator [Slaper et al., 1995]; or (2) adapt the model to the measured data; that entails modeling each spectral data point individually, using the actual solar zenith angle and atmospheric conditions at the moment of the measurement, and convoluting the model spectra with the slit function of the monochromator. A model evaluation by comparison of measured and modeled data is not affected by the choice of the method. The presented investigation follows the second strategy for the following reasons:

1. Both, model and measurement have a finite bandwidth. Deconvolution to an ideal bandwidth of zero is limited by the uncertainties of both data sets, and deconvolution algorithms like the one proposed by Slaper et al. [1995] are based on a certain extraterrestrial spectrum and might bias the comparison of model and measurement. The best solution is therefore to convolute the higher resolved model spectrum (0.15 nm FWHM) with the slit function of the monochromator (0.6 nm FWHM) which is already very low considering the purpose of the measurement: The error in DNA-weighted irradiance [Caldwell et al., 1986] resulting from the bandwidth of our monochromator is less than 1%. The experimental bandwidth is therefore no severe limitation for the determination of biological effects.

2. Varying solar zenith angle and atmospheric conditions can easily be considered, if the exact time for each single data point is known. Modeling each data point with the actual input parameters reduces the uncertainty compared to interpolating the measurements to specified times.

3. One of our main applications for modeling UV irradiance is process studies, for example, by comparison of measured spectra for an aerosol-loaded atmosphere and model spectra for aerosol-free conditions. For these studies we need the spectra which the monochromator would have measured under the desired conditions, which is exactly what our algorithm provides.

Several adaptations are necessary for the realization. First, UVSPEC whose wavelength step is fixed to 1 nm, had to be generalized to arbitrary wavelengths. As model calculation for intervals of 0.25 nm would increase the processor time by a factor of 4, we preferred an algorithm which calculates the intermediate values by interpolation between the 1 nm grid. Due to the low measurement bandwidth of 0.6 nm and the Fraunhofer structure of the solar spectrum, the corresponding model spectrum cannot be constructed by a simple interpolation between data points spaced by 1 nm. This problem has been solved by the following more sophisticated interpolation procedure: In the absence of thermal emission, the solar UV irradiance at the Earth's surface can be written as a product of the extraterrestrial irradiance E_0 of the Sun and the transmittance T_A of the Earth's atmosphere (see Figure 1):

$$E(\lambda) = E_0(\lambda) \cdot T_A(\lambda) \quad (6)$$

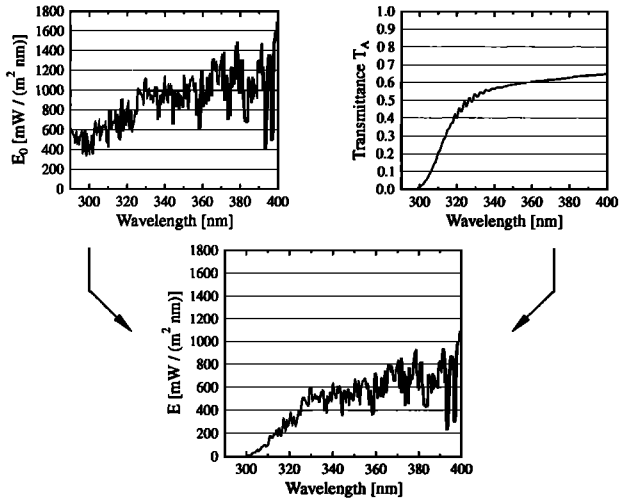


Figure 1. Components of a solar spectrum at the Earth's surface. (Top left) The fine structure, the so-called Fraunhofer lines, is determined by the absorption in the solar atmosphere. (Top right) The processes in the Earth's atmosphere, mainly Rayleigh scattering and ozone absorption, define the transmittance T_A and form the UVB cutoff. (Bottom) The resulting spectrum is the product of the top graphs (equation 6).

While the extraterrestrial irradiance $E_0(\lambda)$ is nearly constant over time in the UVB and UVA (except the annual variation of the Sun-Earth distance which can be calculated and small changes in the emission of the Sun which rarely exceed 1% [Lean, 1991]), the transmittance T_A strongly depends on the composition of the Earth's atmosphere and is therefore highly variable with time. On the other hand, while E_0 is highly variable on the wavelength scale, the transmittance T_A forms a relatively smooth curve (see Figure 1, upper graph). The Fraunhofer structure is formed in the solar atmosphere and is therefore part of the extraterrestrial irradiance E_0 . The processes in the Earth's atmosphere, dominated by ozone absorption and Rayleigh scattering, vary only smoothly with wavelength and determine the absolute value of the irradiance and the UVB cutoff. Consequently, it is sufficient to calculate the transmittance with the UVSPEC step width of 1 nm, interpolate it to an arbitrary wavelength grid, and multiply with a high-resolution extraterrestrial spectrum, in order to achieve a highly resolved model spectrum.

The developed interface SDMODEL is based on exactly this principle. Figure 2 shows the steps necessary for the calculation of a high-resolution model spectrum. Measured spectra are read and split into intervals during which the change of solar zenith angle is less than 0.1° . The diurnal variations of ozone, visibility and Ångström parameters are interpolated to the actual time and used to create an input file for UVSPEC. Calling the model, the transmittance T_A is calculated, interpolated to the wavelengths of the high-resolution extraterrestrial irradiance, multiplied with the extraterrestrial irradiance, and convoluted with the slit function of the monochromator. After correction for the Earth-

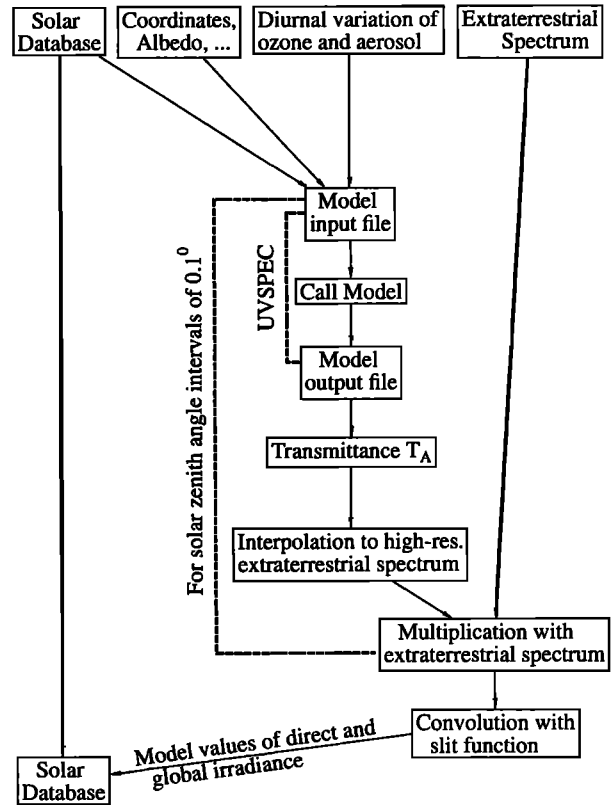


Figure 2. Overview of the SDMODEL algorithm, the interface between model and measurement.

Sun distance, the result is written to the measurement database and can easily be compared with experimental data or used for process studies.

SDMODEL is a flexible tool for comparing model results and measurements. It is easily applicable for other models, as it creates an input file for the model, calls the model and then reads the model output. The processor time depends only little on the wavelength step of the model spectrum and is mainly determined by the time necessary for calculating a single data point. For the present investigations we used the model types TWO-STREAM and PSEUDO-SPHERICAL, the former because of its high speed, the latter because of its accuracy even for high solar zenith angles. The processor time for modeling measurements of 1 day, which amount to about 100 spectra, is 45 min for TWO-STREAM and 3.5 hours for PSEUDO-SPHERICAL (times specified for a Pentium 90 MHz, 16 MByte RAM).

3. Results

A first approach to compare measurement and model is to look at single spectra. Figure 3 shows the ratio of measurement and model for noontime spectra of direct and global irradiance on May 3, 1995. In order to demonstrate the effect of differing bandwidths between experimental and calculated spectra, the upper graph shows the comparison using "raw UVSPEC" with a step width of 1 nm and a bandwidth of 0.15 nm

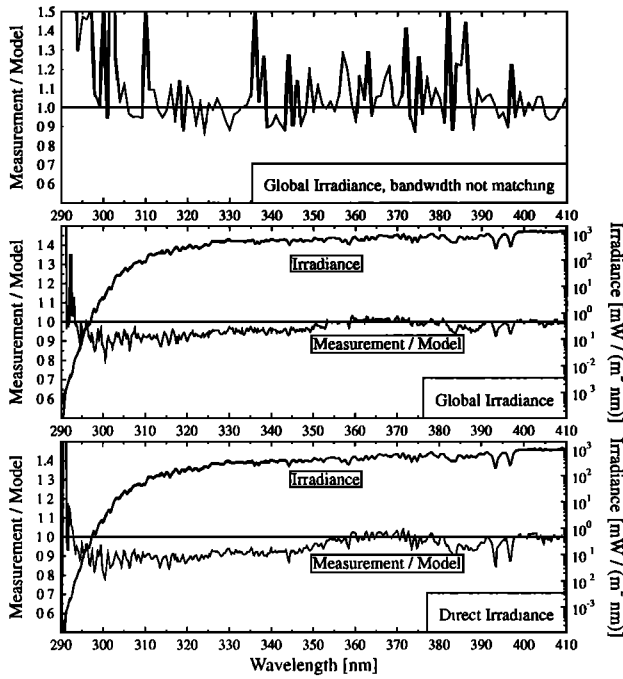


Figure 3. Ratio of measurement and model for May 3, 1995, noontime, solar zenith angle 32° . (Top) Using the original bandwidths of model (0.15 nm) and measurement (0.6 nm), the ratio between both spectra is highly structured. (Middle) The spectra of the global irradiance were corrected for this difference by convoluting the model spectrum with the slit function of the monochromator. (Bottom) Same as middle graph, but for direct irradiance. The remaining structure in the middle and lower graphs is typical for all calculated ratios; the scatter may be due to a small remaining difference in the bandwidths of model and measurement.

which is much smaller than the experimental bandwidth of 0.6 nm. The Fraunhofer absorption lines cause large fluctuations in the ratio which complicate the interpretation of the differences. The middle and lower graphs show SDMODEL results which are automatically corrected for the difference in bandwidth. Both graphs contain absolute irradiance values on a logarithmic scale (right axis) and the ratio between measurement and model (left axis). The fluctuations are much smaller than in the upper graph, indicating the importance of the bandwidth correction. For wavelengths longer than 295 nm, the deviation between model and measurement is generally less than 15%. The low “scatter” of a few percent can be explained by a small remaining difference between the bandwidths of measurement and model. This effect is most pronounced at deep absorption lines like the calcium lines at 393 and 397 nm. The agreement between model and measurement can be considered very good, keeping in mind that the deviation is smaller than 15% over 5 decades of magnitude.

While the comparison of single spectra provides a first quick look at the differences between model and measurement, statistically significant results require the evaluation of a large variety of spectra. From a 2 years’ observation period, we extracted 1200 cloudless

sky spectra as described above. These data cover solar zenith angles between 24° and 80° , ozone column values from 250 to 370 DU and aerosol optical depths at 340 nm from 0 to 0.6. Only data with snow-free surface were chosen for the present analysis. Weighted doses of UV irradiance were calculated using erythema [McKinlay and Diffey, 1987], and DNA damage [Caldwell et al., 1986] action spectra. Figure 4 shows the ratio of measured and calculated erythemally effective doses for different model types. The ratio between measurement and model is plotted as a function of solar zenith angle. Even with the fast TWOSTREAM⁺⁺ model the agreement is quite good (upper graph). A slight dependence on solar zenith angle is obvious, however. The agreement is significantly improved using the slower, but more accurate PSEUDO-SPHERICAL⁺⁺ model (middle graph). The systematic deviation is less than in the TWOSTREAM case; no significant dependence on solar zenith angle can be observed. The lower graph, finally, shows the results for the TWODIS⁺⁺ model which has been described above. This type combines the speed of TWOSTREAM⁺⁺ and, as can be seen in the figure, the accuracy of PSEUDO-SPHERICAL⁺⁺. Table 1 shows averages as well as standard deviations of the measurement to model ratio for the three model types shown in

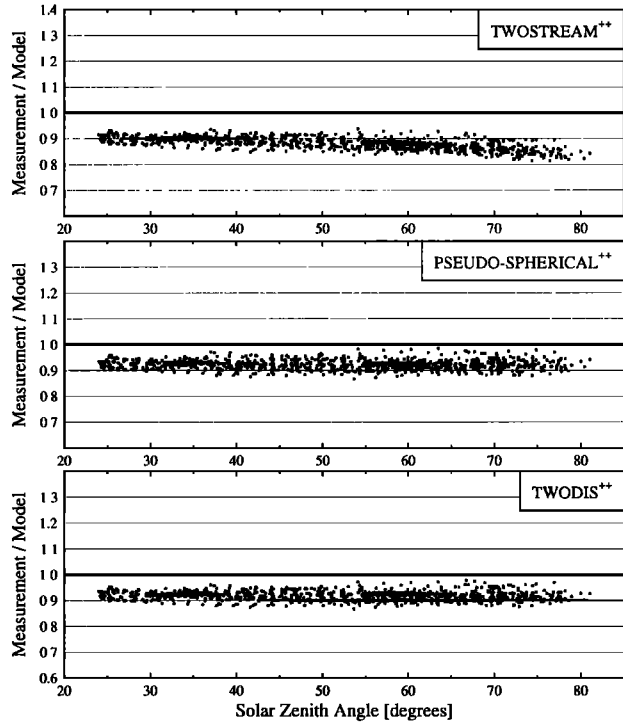


Figure 4. Ratio of measured and modeled erythema irradiances for (top) TWOSTREAM⁺⁺, (middle) PSEUDO-SPHERICAL⁺⁺, and (bottom) TWODIS⁺⁺. The fast TWOSTREAM⁺⁺ model shows systematic deviations, especially for large solar zenith angles; PSEUDO-SPHERICAL⁺⁺ results are much better. TWODIS⁺⁺, which combines the speed of TWOSTREAM⁺⁺ with the accuracy of PSEUDO-SPHERICAL⁺⁺, is hardly distinguishable from PSEUDO-SPHERICAL⁺⁺.

Table 1. Average and Standard Deviation for the Ratio of Measurement and Model for All 1200 Spectra

Model Type	Average	Standard Deviation
<i>UVA (315 - 400 nm)</i>		
TWOSTREAM ⁺⁺	0.947	0.031
PSEUDO-SPHERICAL ⁺⁺	0.961	0.030
TWODIS ⁺⁺	0.956	0.028
<i>UVB (280 - 315 nm)</i>		
TWOSTREAM ⁺⁺	0.855	0.037
PSEUDO-SPHERICAL ⁺⁺	0.910	0.020
TWODIS ⁺⁺	0.907	0.020
<i>CIE Erythema</i>		
TWOSTREAM ⁺⁺	0.879	0.023
PSEUDO-SPHERICAL ⁺⁺	0.922	0.019
TWODIS ⁺⁺	0.918	0.018
<i>DNA Damage</i>		
TWOSTREAM ⁺⁺	0.855	0.026
PSEUDO-SPHERICAL ⁺⁺	0.912	0.022
TWODIS ⁺⁺	0.908	0.024

Figure 4 and different weighting functions or spectral ranges. The systematic deviation results from systematic uncertainties in the model input (mainly the extraterrestrial spectrum) and the measurement (mainly the absolute calibration). The standard deviation is determined by the statistical errors of the measurement and the input parameters as well as changes in the profiles of ozone and aerosol extinction which are not considered explicitly but defined by means of standard profiles. The statistical uncertainty of the calibration of our spectroradiometric system has been found to be $\pm 2.1\%$ ($\pm 1\sigma$) for erythemal irradiance and $\pm 1.5\%$ for UVA irradiance, which explains a good part of the standard deviation observed for the PSEUDO-SPHERICAL⁺⁺ and TWODIS⁺⁺ models.

The results for the PSEUDO-SPHERICAL⁺⁺ model are summarized in Figure 5. The upper and middle graphs show the ratio of model and measurement for UVA and erythemally weighted irradiance. To characterize the spectral dependence of the ratio, data were grouped in solar zenith angle intervals of 10° and wavelength intervals of 10 nm; the lower graph in Figure 5 shows the average and standard deviation for these groups of data. For wavelengths larger than 295 nm, the deviation between measurement and model is smaller than 11%, which is comparable to the differences observed for good instruments during intercomparison campaigns [McKenzie *et al.*, 1993; Gardiner and Kirsch, 1995; Seckmeyer *et al.*, 1995]. The variation of the ratio with solar zenith angle is quite low, especially in the UVB range.

Modeling direct spectral irradiance is much easier from the numerical point of view, since only the attenuation according to the Bouguer-Lambert-Beer law has to be considered. On the other hand, direct irradiance is much more sensitive to attenuation by aerosols and therefore subject to uncertainties in the determination of the aerosol optical depth, and the numerical treat-

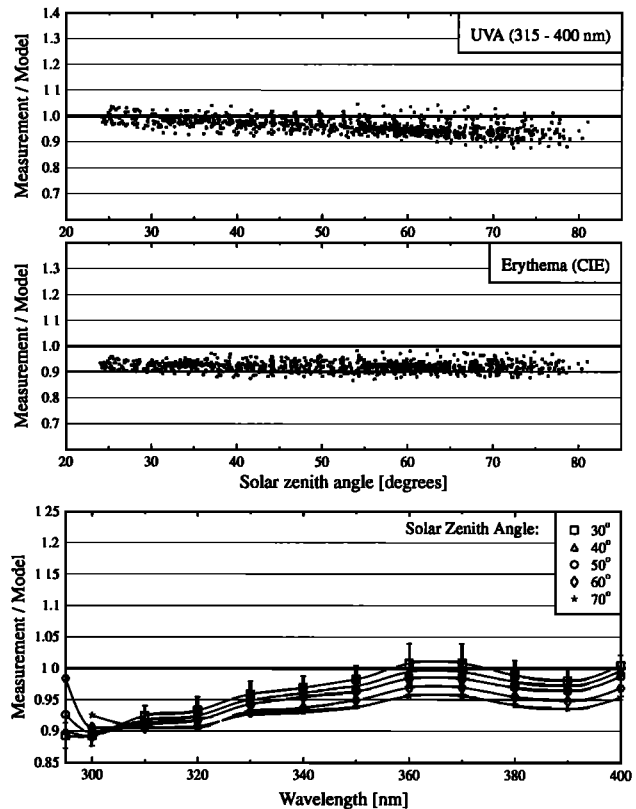


Figure 5. PSEUDO-SPHERICAL⁺⁺ results. Ratio between measurement and model for (top) UVA and (middle) erythemally weighted irradiance and (bottom) as a function of wavelength and solar zenith angle where data were averaged over intervals of 10° solar zenith angle and 10 nm wavelength. The error bars correspond to $\pm 1\sigma$ for 30° solar zenith angle.

ment of this parameter within the model. Global irradiance is less sensitive, as the reduction of direct irradiance is partly compensated by enhanced scattered irradiance. Figure 6 shows the results of direct irradiance calculated by TWOSTREAM (the calculation of the direct spectral irradiance is identical for TWOSTREAM and PSEUDO-SPHERICAL). The large deviation of up to 40% in the upper graph results from the nonideal parameterization of the aerosols using visibility (see above). Significantly better results are achieved with the modified model version TWOSTREAM⁺⁺ (middle graph) which uses the Ångström parameterization. The standard deviation of 21% observed with TWOSTREAM is reduced to 6% with TWOSTREAM⁺⁺. It must be noted here that in contrast to the investigations of global irradiance, model input (ozone column and aerosol optical depth) and output (direct irradiance) are not independent, because direct irradiance is used for the determination of the input parameters. Although this might indicate a better agreement between model and measurement in the direct irradiance case, a similar structure as in the global case can be observed in the ratio (lower graph, Figure 6). The curve does hardly depend on solar zenith angle. A deviation, almost identical for global and direct irradiance and nearly inde-

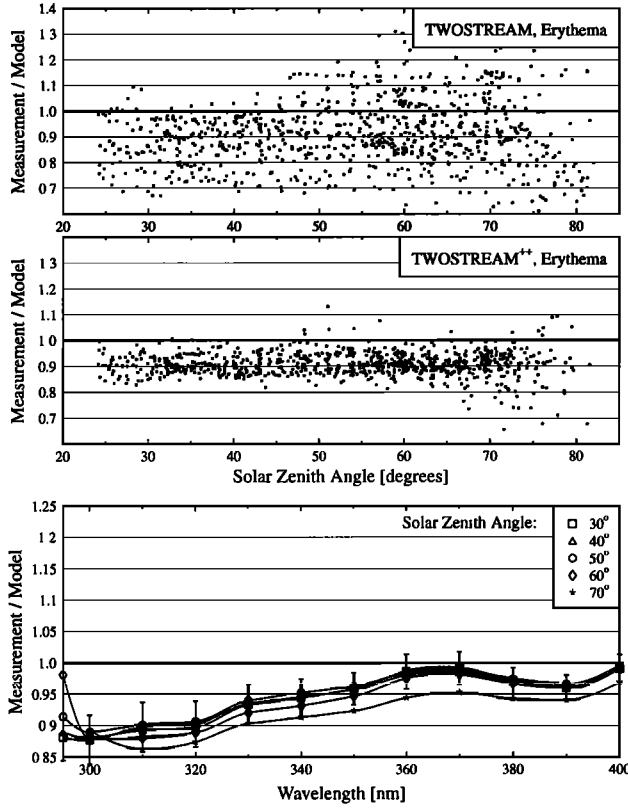


Figure 6. Ratio between measurement and model for the direct spectral irradiance for (top) TWOSTREAM, (middle) TWOSTREAM⁺⁺, and (bottom) TWOSTREAM⁺⁺ as a function of wavelength and solar zenith angle where data were averaged over intervals of 10° solar zenith angle and 10 nm wavelength. Using TWOSTREAM large scatter is observed; the largest deviations occur at high aerosol optical depths, indicating that the aerosol parameterization via visibility is not sufficient in the UV range. The result is much better when the TWOSTREAM⁺⁺ model is used instead.

pendent of solar zenith angle, leaves only a few possible explanations. On the model side, this is the extraterrestrial irradiance (ATLAS 3). A general error analysis for these data is not available, but for the previously measured spectrum (ATLAS 2), the accuracy is specified to be 4–8% [Woods et al., 1996]. On the experimental side there are different sources of error, comprising mainly the uncertainty of the absolute calibration standard which is typically specified as 4%, possible nonlinearities of the system, and the remaining uncertainty after correction of the cosine error of the entrance optics [Seckmeyer and Bernhard, 1993] (the latter is unlikely to be the cause for the observed wavelength dependence, because the measurement of direct irradiance is not subject to the cosine error). The observed deviation of less than 11% can therefore be explained by the systematic errors of both measurement and model.

In order to show the importance of correct treatment of aerosols for modeling global irradiance, Figure 7 shows the erythemally weighted irradiance calculated

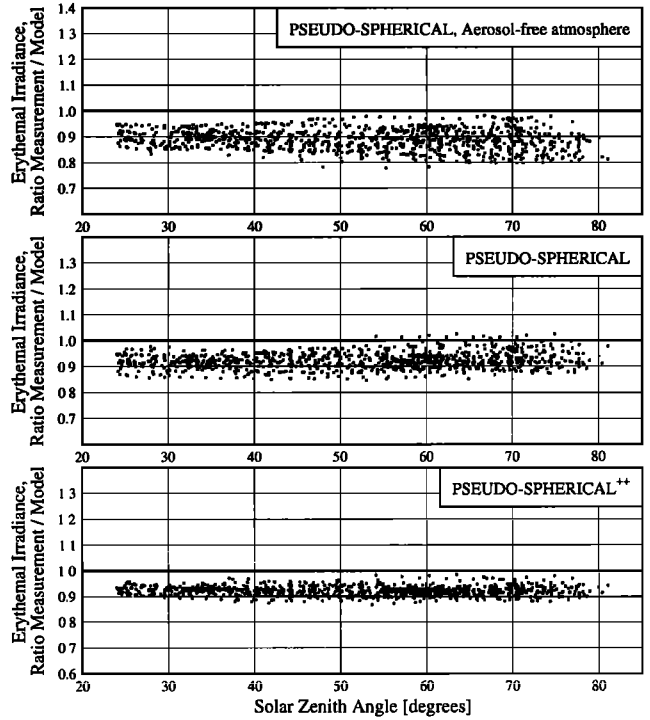


Figure 7. Influence of atmospheric aerosols on the ratio between measured and modeled erythemally weighted global irradiance. (Top) Results of PSEUDO-SPHERICAL without consideration of aerosols in the model input show that the model clearly overestimates the measured results as it does not consider the reduction due to aerosols. (Middle) The agreement is improved when aerosols are included into the model calculations. (Bottom) The smallest deviation between model and measurement is achieved using PSEUDO-SPHERICAL⁺⁺ where aerosols are parameterized by the Ångström turbidity parameters.

with PSEUDO-SPHERICAL using different aerosol parameterizations. Omitting scattering by aerosols in the model (upper graph) leads to a systematic overestimation of the global irradiance. Better agreement is achieved when specifying the visibility derived from the measured Ångström parameters with equation (1) (middle graph). There is still a random error, but a much lower one than in the direct irradiance case (see upper graph of Figure 6). This reflects the above mentioned fact that the global irradiance is less sensitive to the aerosol optical depth. Using the Ångström parameterization (model type PSEUDO-SPHERICAL⁺⁺ in the lower graph of Figure 7) reduces the relative standard deviation of the ratio from 3.2% in the PSEUDO-SPHERICAL case to only 1.9%. This indicates that the Ångström parameters provide a sufficient description of the aerosol optical depth in the UV range. The aerosols at the rural IFU site are mainly of the non-absorbing kind (water vapor). Insufficient description of aerosols may therefore provide larger deviations at urban sites with higher aerosol optical depths and a larger fraction of absorbing aerosols. For such locations it might be necessary to additionally specify the sin-

gle scattering albedo, the experimental determination of which is much more complicated than that of the spectral optical depth.

Finally, Figure 8 shows the ratio of direct and global irradiance for May 7, 1994. This ratio can be used for sensitivity studies of the profiles of ozone and aerosol attenuation if they are available [Zeng *et al.*, 1994]. The ratio is affected neither by the error in the absolute calibration of the measurement system, nor by the uncertainty of the extraterrestrial spectrum. In order to calculate the ratio, both spectra had to be interpolated to the same solar zenith angle. Figure 8 shows quite a good agreement between modeled and measured ratio for all solar zenith angles. It is interesting to note that in the UVB range, in contrast to the UVA and visible, direct irradiance contributes always less than 50% to the global irradiance, even for a clear day like May 7, 1994, when the aerosol optical depth at 340 nm did not exceed 0.15.

4. Summary and Conclusions

One of the main goals of our presentation was to show how a comparison between measurement and model can be performed. SDMODEL, the tool that has been developed for this purpose, can also be used for a wide range of investigations, so-called process studies. In particular, these are all kinds of studies where experimental data are to be compared with model values calculated for specific atmospheric conditions, like, for example, a cloudless aerosol-free sky. The developed tool has been used to compare measurement and model for 1200 cloudless sky spectra, gathered during 2 years of continuous measurements at the IFU site. These studies lead to the following conclusions:

1. Using the SDMODEL interface, the UVSPEC model package has been evaluated for the IFU site.

The comparison with 2 years of experimental cloudless sky data showed very good agreement between measurement and model. For the PSEUDO-SPHERICAL model type, the systematic deviations in spectral irradiance ranged between -11 and +2% for wavelengths between 295 and 400 nm and solar zenith angles up to 80°.

2. The observed deviations between model and measurement are fully explained by the uncertainties of both measurement and model. The systematic difference of 11% is due to errors of the model input parameters (e.g., the extraterrestrial irradiance) and the absolute calibration of the spectroradiometer, possible small nonlinearities of the system, and the remaining uncertainty after correction of the cosine error of the entrance optics. The statistical uncertainty of 2-3% is explained by the experimental uncertainty between subsequent calibrations and the variation of parameters that were not explicitly considered by the model (e.g. the ozone profile).

3. Some improvements are possible concerning the extraterrestrial irradiance. Before ATLAS 3 became available, we used ATLAS 2 [Woods *et al.*, 1996], which gave a slightly better agreement on the absolute scale (systematic difference between measurement and model smaller than $\pm 6\%$). The absolute uncertainty of ATLAS 2 is specified as 4-8%. On the wavelength scale, however, we found deviations of between 0.1 and 0.2 nm for ATLAS 2, compared to our mercury lamp calibration which is accurate to 0.05 nm. We therefore decided to use ATLAS 3, which agrees with our wavelength scale within the uncertainty of the measurement.

4. The agreement between model and measurement was improved using a slightly modified (++) version of UVSPEC which uses the Ångström parameterization for the aerosols instead of visibility. This is due to the better representation of the wavelength dependence of the aerosol optical depth.

5. It has been shown that the knowledge of ozone column and spectral aerosol depth parameterized by the Ångström formula is sufficient to achieve this good level of agreement for a cloudless sky. The majority of input parameters may therefore either be taken from standard profiles (e.g., the ozone and aerosol profiles) or set as constant (e.g., ground albedo and surface pressure). Ground albedo is another important input parameter if measurements over snow-covered surfaces are considered.

6. Without the knowledge of aerosol optical depth the systematical and statistical deviations between model and measurement increase significantly.

7. A new model type TWODIS has been defined in order to combine the advantages of the fast TWO-STREAM and the accurate PSEUDO-SPHERICAL algorithms. By comparison with experimental data it has been shown that a properly used two-stream code may reach an accuracy comparable to a discrete ordinate multistream model.

8. The model has been evaluated for the IFU site, which encounters a wide range of atmospheric conditions and solar zenith angles. Further studies are re-

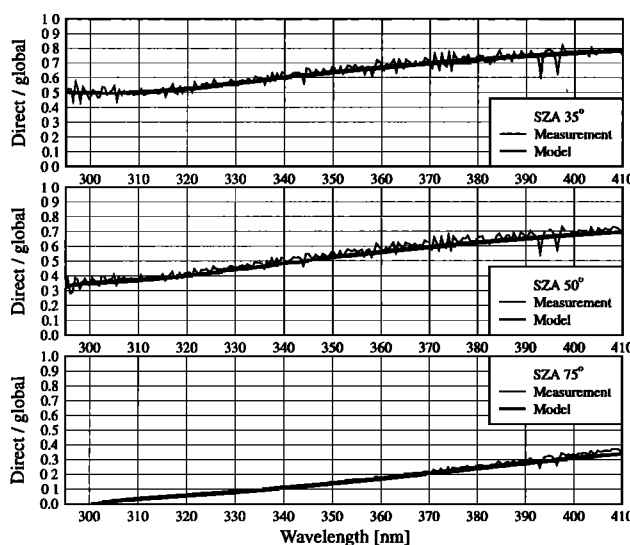


Figure 8. Ratio between direct and global irradiance, measured on May 7, 1994, in comparison with modeled (PSEUDO-SPHERICAL⁺⁺) values for solar zenith angles (SZA) of 35°, 50°, and 75°.

quired, however, to generalize the presented results to other locations with different conditions like, for example, urban areas with more absorbing aerosols. For such locations it might be necessary to additionally specify the single scattering albedo, the experimental determination of which is much more complicated than that of the spectral optical depth.

9. The evaluated model together with the newly developed interface may be used for detailed investigations of the influence of several parameters like aerosols, surface albedo and clouds. A possible procedure for these studies could be the comparison of experimental data with appropriate model values.

UVSPEC, a program for calculation of diffuse and direct UV and visible fluxes and intensities at any altitude is available by anonymous ftp to pluto.itek.norut.no, cd /pub/arve. UVSPEC will soon be replaced by the much improved, user friendly and flexible Radtran program. It will be available from the same location as UVSPEC.

Appendix: Determination of Atmospheric Parameters From Direct Spectral Irradiance

Attenuation of direct solar irradiance E_{dir} within the Earth's atmosphere can be described by the Bouguer-Lambert-Beer law. This formula which is utilized by the standard methods for the determination of ozone, the Dobson and Brewer methods in particular, is also used with the DSI (direct spectra interpretation) algorithm described here. Mainly three processes control direct UV irradiance, namely Rayleigh scattering, aerosol extinction and absorption by ozone. Other trace gases than ozone, e.g., SO₂, may be of importance in highly polluted urban areas, but not at IFU (U. Köhler, personal communication, 1996). According to the Bouguer-Lambert-Beer law, the total optical depth therefore is expressed as

$$-\ln \left(\frac{E_{dir}}{E_0} \right) = m_{Rayleigh} \cdot \tau_{Rayleigh} + m_{aerosol} \cdot \tau_{aerosol} + m_{ozone} \cdot \tau_{ozone} \quad (A1)$$

where E_0 is the extraterrestrial irradiance and m the so-called optical mass, a factor that considers the slant path of the radiation through the atmosphere. The optical masses, which to a first approximation equal $1/\cos\theta$ (θ is the solar zenith angle) are calculated according to a formula described by Thomason *et al.* [1983]. The necessary input parameters for these calculations, standard profiles of pressure, temperature and ozone concentration are taken from the U.S. standard atmosphere [Anderson *et al.*, 1986]. The left side of equation (A1) can be calculated from the measured direct spectral irradiance E_{dir} and the extraterrestrial irradiance E_0 , in this case the ATLAS 2 spectrum [Woods *et al.*, 1996] convoluted with the slit function of the monochromator. To separate the three components $\tau_{Rayleigh}$, $\tau_{aerosol}$, and τ_{ozone} on the right side, their specific wavelength dependence is utilized. The Rayleigh optical depth is calculated using the formula of

Teillet [1990]. After correction for Rayleigh scattering, aerosol extinction is determined at wavelengths greater than 330 nm where ozone absorption is negligible. An Ångström turbidity formula $\tau_{Angström} = \beta \cdot \lambda^{-\alpha}$ is fitted to the data to parameterize aerosol extinction (λ is the wavelength in micrometer). After correction for the Rayleigh scattering and aerosol contribution using the Ångström formula for the whole UV range, only ozone absorption is left. The ozone column can be calculated by linear regression of τ_{ozone} versus the absorption cross section of ozone, evaluated at each measured wavelength, considering the temperature dependence of the cross section with a standard temperature profile. Figure 9 shows a typical example for the described procedure. The Ångström formula provides a good description for the observed aerosol optical depth. The small residual shows that the three processes (Rayleigh scattering, aerosol extinction and ozone absorption) can explain the measured optical depth quantitatively.

The advantage of the method compared to common ozone measurements is that additional information about the aerosol optical depth is obtained, which is an important input parameter for modeling UV irradiance at the Earth's surface. DSI reduces the uncertainty of the ozone determination using a complete spectrum of 500 data points for the analysis. Problems like the change of solar zenith angle during the measurement are simply avoided by the algorithm which calculates the optical mass separately for each spectral data point. A related method is described by Huber *et*

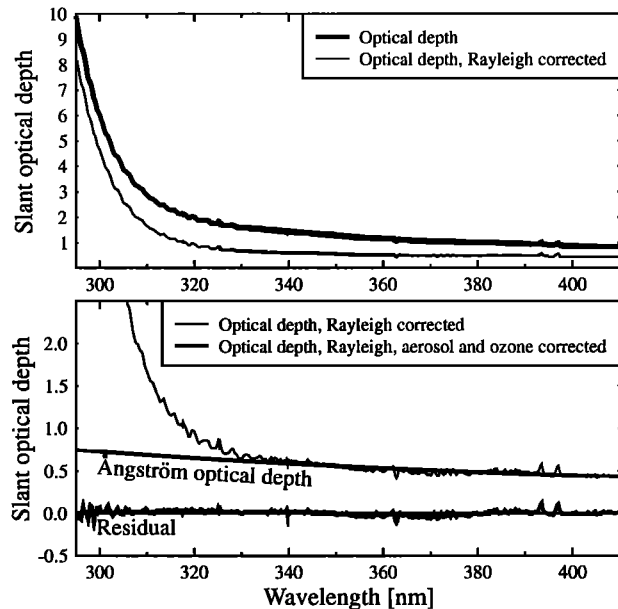


Figure 9. Calculation of ozone column and aerosol optical depth with DSI, August 1, 1995, solar zenith angle 34°. (Top) Slant optical depth (calculated from the ratio of measured direct versus extraterrestrial irradiance) and Rayleigh-corrected slant optical depth. (Bottom) Rayleigh-corrected optical depth and the fitted Ångström turbidity formula. The residual after correction for Rayleigh, aerosol and ozone equals zero to a good approximation.

al. [1995] where measured direct spectral irradiance is compared with model calculations to derive ozone column and aerosol optical depth.

In order to estimate the accuracy of the developed algorithm, the DSI results were compared with Brewer measurements of Hohenpeissenberg (U. Köhler, personal communication, 1996), a site of the German Weather Service about 40 km to the north of IFU. For more than 500 data points, sampled over half a year, we found a systematic deviation of only 1% (IFU data were higher) and a standard deviation of the ratio of 1.6%. These small differences are a combined effect of the uncertainties of both algorithms and real differences arising from the unavoidable distance in space (40 km) and time.

Acknowledgments. We thank Astrid Albold, German Bernhard and Edeltraud Leibrock for carefully reading the manuscript and for their valuable comments. This work has been funded by the German Ministry for Science, Education, Research, and Technology (BMBF) and the European Comission, DG XII within the framework of the SUVDAMA project. One of us (A.K.) would like to thank the National Aeronautics and Space Administration for support to develop UVSPEC through grant NAGW-2165 to the University of Alaska-Fairbanks.

References

- Anderson, G.P., S.A. Clough, F.X. Kneizys, J.H. Chetwynd, and E.P. Shettle, AFGL atmospheric constituent profiles (0-120 km), *Tech. Rep. AFGL-TR-86-0110*, Air Force Geophys. Lab., Hanscom Air Force Base, Mass., 1986.
- Blumthaler, M., and W. Ambach, Solar UVB-albedo of various surfaces, *Photochem. Photobiol.*, **48**, 85-88, 1988.
- Blumthaler, M., J. Gröbner, M. Huber, and W. Ambach, Measuring spectral and spatial variations of UVA and UVB sky radiance, *Geophys. Res. Lett.*, **23**, 547-550, 1996.
- Caldwell, M.M., L.B. Camp, C.W. Warner, and S.D. Flint, Action Spectra and Their Role in Assessing Biological Consequences of Solar UV-B Radiation Change, in *Stratospheric Ozone Reduction, Solar Ultraviolet Radiation and Plant Life, NATO ASI ser.*, vol. G8, edited by R.C. Worrest and M.M. Caldwell, Springer-Verlag, New York, pp. 87-111, 1986.
- Dahlback, A., and K. Stamnes, A new spherical model for computing the radiation field available for photolysis and heating at twilight, *Planet. Space Sci.*, **39**, 671-683, 1991.
- Daumont, D., J. Brion, J. Charbonnier, and J. Malicet, Ozone UV spectroscopy, I, Absorption cross-sections at room temperature, *J. Atm. Chem.*, **15**, 145-155, 1992.
- Forster, P.M.F., P.K. Shine, and A.R. Webb, Modeling ultraviolet radiation at the Earth's surface, II, Model and instrument comparison, *Journal of Applied Meteorology*, **34**, 2426-2439, 1995.
- Gardiner, B.G., and P.J. Kirsch, Second European intercomparison of ultraviolet spectrometers, Panorama, Greece, 21-31 August 1992, Report to the Commission of the European Communities, contract STEP CT900076, Brussels, Belgium, 1993.
- Gardiner, B.G., and P.J. Kirsch, Setting standards for European ultraviolet spectroradiometers. Report to the Commission of the European Communities, contract STEP CT900076, Brussels, Belgium, 1995.
- Gardiner, B.G., et al., European intercomparison of ultraviolet spectroradiometers, *Environ. Technol.*, **14**, 25-43, 1993.
- Harris, N.R.P., et al., *UNEP/WMO Scientific Assessment of Ozone Depletion*, chap. 1, Ozone measurements, United Nations Econ. Programme, Nairobi, Kenya, 1995.
- Huber, M., M. Blumthaler, W. Ambach, and J. Staehelin, Total atmospheric ozone determined from spectral measurements of direct solar UV irradiance, *Geophys. Res. Lett.*, **22**, 53-56, 1995.
- Iqbal, M., *An Introduction to Solar Radiation*, Academic, San Diego, Calif., 1983.
- Koskela, T., and P. Taalas, Measured and modeled UV-B spectrum compared with some atmospheric parameters, in *Atmospheric Radiation*, edited by K. Stamnes, *SPIE Proc. Int. Soc. Opt. Eng.*, **2049**, 296-306, 1993.
- Kylling, A., K. Stamnes, and S.-C. Tsay, A reliable and efficient two-stream algorithm for spherical radiative transfer: Documentation of accuracy in realistic layered media, *J. Atm. Chem.*, **21**, 115-150, 1995.
- Lean, J., Variations in the Sun's radiative output, *Rev. Geophys.*, **29**, 505-535, 1991.
- Lenoble, J. *Atmospheric Radiative Transfer*. A. DEPAK, Hampton, Va., 1993.
- Mayer, B., and G. Seckmeyer, All-weather comparison between spectral and broadband (Robertson-Berger) UV measurements, *Photochem. Photobiol.*, **64**, 792-799, 1996.
- McKenzie, R.L., M. Kotkamp, G. Seckmeyer, R. Erb, C.R. Roy, H.P. Gies, and S.J. Toomey, First southern hemisphere intercomparison of measured solar UV spectra, *Geophys. Res. Lett.*, **20**, 2223-2226, 1993.
- McKenzie, R.L., M. Blumthaler, C.R. Booth, S.B. Diaz, J.E. Frederick, T. Ito, S. Madronich, and G. Seckmeyer, *UNEP/WMO Scientific Assessment of Ozone Depletion*, chap. 9, Surface Ultraviolet Radiation, United Nations Econ. Programme, Nairobi, Kenya, 1995.
- McKinlay, A.F. and B.L. Diffey, A reference action spectrum for ultraviolet induced erythema in human skin, *CIE J.*, **6**, 17-22, 1987.
- Nicolet, M., On the molecular scattering in the terrestrial atmosphere: An empirical formula for its calculation in the homosphere, *Planet. Space Sci.*, **32**, 1467-1468, 1984.
- Ruggaber, A., R. Dlugi, and T. Nakajima, Modeling of radiation quantities and photolysis frequencies in the troposphere, *J. Atm. Chem.*, **18**, 171-210, 1994.
- Seckmeyer, G. and G. Bernhard, Cosine error correction of spectral UV irradiances, in *Atmospheric Radiation*, edited by K. Stamnes, *SPIE Proc. Int. Soc. Opt. Eng.*, **2049**, 140-151, 1993.
- Seckmeyer, G., et al., First intercomparison of spectral UV-radiation measurement systems, *Appl. Opt.*, **33**, 7805-7812, 1994.
- Seckmeyer, G., et al., Geographical differences in the UV measured by intercompared spectroradiometers, *Geophys. Res. Lett.*, **22**, 1889-1892, 1995.
- Seckmeyer, G., G. Bernhard, B. Mayer, and R. Erb, High accuracy spectroradiometry of solar UV radiation, *Meteorologia*, **32**, 697-700, 1996.
- Shettle, E.P., Models of aerosols, clouds and precipitation for atmospheric propagation studies, In *Atmospheric propagation in the UV, visible, IR and mm-region and related system aspects*, *ÅGARD Conf. Proc.*, pp. 15-1-15-13, 1989.
- Slaper, H., H.A.J.M. Reinen, M. Blumthaler, M. Huber, and F. Kuik, Comparing ground-level spectrally resolved solar UV measurements using various instruments: A technique resolving effects of wavelength shift and slit width, *Geophys. Res. Lett.*, **22**, 2721-2724, 1995.

- Stamnes, K., The theory of multiple scattering of radiation in plane parallel atmospheres, *Rev. Geophys.*, **24**, 299–310, 1986.
- Stamnes, K., S.C. Tsay, W. Wiscombe , and K. Jayaweera, A numerically stable algorithm for discrete-ordinate-method radiative transfer in multiple scattering and emitting layered media, *Appl. Opt.*, **27**, 2502–2509, 1988.
- Teillet, P., Rayleigh optical depth comparisons from various sources, *Appl. Opt.*, **29**, 1897–1900, 1990.
- Thomason, L.W., B.M. Herman, and J.A. Reagan, The effect of atmospheric attenuators with structured vertical distributions on air mass determinations and Langley plot analysis, *J. Atm. Sci.*, **40**, 1851–1854, 1983.
- Wang, P. and J. Lenoble, Comparison between measurements and modeling of UV-B irradiance for clear sky: a case study, *Appl. Opt.*, **33**, 3964–3971, 1994.
- Woods, T.N., et al., Validation of the UARS solar ultraviolet irradiances: Comparison with the ATLAS 1 and 2 measurements, *J. Geophys. Res.*, **101**, 9541–9569, 1996
- Zeng, J., R.L. McKenzie, K. Stamnes, M. Wineland, and J. Rosen, Measured UV spectra compared with discrete ordinate method simulations, *J. Geophys. Res.*, **99**, 23019–23030, 1994.
-
- B. Mayer and G. Seckmeyer, Fraunhofer Institute for Atmospheric Environmental Research, Kreuzeckbahnstrasse 19, D-82467 Garmisch-Partenkirchen, Germany. (email: mayer@ifu.fhg.de; seck@ifu.fhg.de)
- A. Kylling, NORUT Information Technology, N-9005 Tromsø, Norway. (email: arve.kylling@itek.norut.no)

(Received September 9, 1996; revised January 17, 1997; accepted January 17, 1997.)